

Efficient Calibration of Industrial Robots in Multi-Spherical Constraints

Supplementary Material

Anonymous

This supplementary file contains several figures and tables related to symbols, experiments, and kinematic parameters, as well as the complete convergence proof of the MSCA algorithm and the IEKF-MSCA's pseudocode.

I. ADDITIONAL TABLES

TABLE S.I. SYMBOL LIST.

| Symbol | Explanation |
|--|---|
| Y_i | Transformation matrix. |
| a, α, θ, d | Link length, link twist angle, link offset, joint angle. |
| B, S | Rotation matrix, position vector. |
| dY | Holomorphic differential Y . |
| ΔE | Kinematic error. |
| H | Jacobian matrix of the kinematic error model. |
| ΔO | Kinematic parameters error vector. |
| $\Delta \alpha, \Delta a, \Delta \theta, \Delta d$ | Vector of the kinematic parameter deviations. |
| L | Loss function. |
| \hat{V}, V | Theoretical and measured draw-wire lengths. |
| Z | Fixed point on the ground. |
| $S(O)$ | Theoretical robot end-effector position |
| M | Sample count (measurement configurations). |
| O | D-H parameter vector. |
| Q | Covariance matrix of system noise. |
| v_k | Measurement noise. |
| I | Unit matrix. |
| μ | Regularization parameter. |
| a_6, a'_6 | Initial and defined value of the sixth axis link length. |
| Δb | Difference between the length of the dial gauge body and its real-time reading. |
| Φ | Spherical constraint equation. |
| S_i^u | The i -th position on the u -th sphere. |
| ζ^u | The u -th sphere's center. |
| R_u | The radius of the u -th sphere. |
| U | Total number of spheres. |
| $\langle \cdot \rangle$ | The inner product between two matrices |
| κ_u | Constraint coefficient of sphere u . |
| η^u | The coefficient of the Lagrange multiplier for the u -th sphere |
| O_0, Z_0, γ_0 | Initial values of O , Z , and γ . |
| T | Maximum iteration per time step in the IEKF step. |
| C_1 | Maximum iteration to Z in the MSCA step. |
| C_2 | Maximum iteration for updating ζ^u , O and γ^u in the MSCA step. |
| $\{q_{i,1}, \dots, q_{i,6}\}$ | Six robotic rotation angles. |

TABLE S. II. THE D-H PARAMETERS OF AN HRS JR680 ROBOT.

| oint i | $\Delta \alpha_i / ^\circ$ | $\Delta a_i / mm$ | $\Delta d_i / mm$ | $\Delta \theta_i / ^\circ$ |
|----------|----------------------------|-------------------|-------------------|----------------------------|
| 1 | -90 | 250 | 653.5 | 0 |
| 2 | 0 | 900 | 0 | -90 |
| 3 | -90 | -205 | 0 | 180 |
| 4 | 90 | 0 | 1030.2 | 0 |
| 5 | -90 | 0 | 0 | 90 |
| 6 | 0 | 0 | 200.6 | 0 |

TABLE S.III. WILCOXON SIGNED-RANK TEST RESULTS FOR RMSE/MEAN/MAX FROM TABLE III.

| Comparison | <i>p-value</i> | <i>R-</i> | <i>R+</i> |
|-------------------|-----------------------|------------------|------------------|
| M12 vs. M1 | 0.002 | 0 | 45 |
| M12 vs. M2 | 0.002 | 0 | 45 |
| M12 vs. M3 | 0.002 | 0 | 45 |
| M12 vs. M4 | 0.002 | 0 | 45 |
| M12 vs. M5 | 0.002 | 0 | 45 |
| M12 vs. M6 | 0.002 | 0 | 45 |
| M12 vs. M7 | 0.002 | 0 | 45 |
| M12 vs. M8 | 0.002 | 0 | 45 |
| M12 vs. M9 | 0.002 | 0 | 45 |
| M12 vs. M10 | 0.002 | 0 | 45 |
| M12 vs. M11 | 0.002 | 0 | 45 |

* The significance level for acceptance is set at 0.05.

TABLE S.IV. CALIBRATED D-H PARAMETER DEVIATIONS BY THE IEKF-MSCA ON D3.

| Joint <i>i</i> | $\Delta\alpha_i/^\circ$ | $\Delta a_i/mm$ | $\Delta d_i/mm$ | $\Delta\theta_i/^\circ$ |
|-----------------------|---|-----------------------------------|-----------------------------------|---|
| 1 | -0.0547 | 0.0666 | -0.9070 | 0.0043 |
| 2 | 0.0786 | -0.6735 | -0.6355 | -0.0409 |
| 3 | 0.0538 | 0.7865 | -0.6356 | 0.0424 |
| 4 | -0.0055 | 0.7870 | 0.6167 | 0.0048 |
| 5 | 0.0001 | 0.0064 | -0.6357 | 0.0073 |
| 6 | 0.0000 | -0.5577 | 0.9913 | 0.0000 |

II. ADDITIONAL ALGORITHM PSEUDOCODE

| Algorithm I: IEKF-MSCA | | |
|---|--|--------------|
| Input: $O_0, N, \{q_{i,1}, q_{i,2}, \dots, q_{i,6}\}, \{\hat{V}_1, \hat{V}_2, \dots, \hat{V}_N\}$ | | |
| Operation | | Cost |
| /* Initialization */ | | |
| 1. initialize $O_0=O, U=3, Z=Z_0, \xi^{\alpha t}=\xi_0^{\alpha}, \gamma=\gamma_0$ | | $\Theta(1)$ |
| /* IEKF Step */ | | |
| 2. for k to C_0 | | $\times C_0$ |
| 3. set Q_k known | | $\Theta(1)$ |
| 4. set and M_k known | | $\Theta(1)$ |
| 5. calculating $O_{k/k-1}$ via (9) | | $\Theta(1)$ |
| 6. calculating $P_{k/k-1}$ via (9) | | $\Theta(1)$ |
| 7. for i to N | | $\times N$ |
| 8. for $j=1$ to T | | $\times T$ |
| 9. calculate K_k^j via (10) | | $\Theta(1)$ |
| 10. update O_{j+1k} via (11) | | $\Theta(1)$ |
| 11. update P_{j+1k} via (11) | | $\Theta(1)$ |
| 12. $k=k+1$ | | $\Theta(1)$ |
| Output O_{j+1k} | | |
| /* MSCA Step */ | | |
| Input $O_{IEKF}=O_{j+1k}$ | | |
| 13. for $t=1$ to C_1 | | $\times C_1$ |
| 14. for $i=1$ to N | | $\times N$ |
| 15. update Z_{t+1} with (17) | | $\Theta(1)$ |
| 16. $t=t+1$ | | $\Theta(1)$ |
| 17. for $t=1$ to C_2 | | $\times C_2$ |
| 18. for $i=1$ to N | | $\times N$ |
| 19. update $\xi_{u,t+1}$ with (18), $u \in \{1,2,3\}$ | | $\Theta(1)$ |
| 20. update O_{t+1} with (19) | | $\Theta(1)$ |
| 21. update $\gamma_{u,t+1}$ with (20) | | $\Theta(1)$ |
| 22. $t=t+1$ | | $\Theta(1)$ |
| /* Operation Ending */ | | |
| Output: O | | |

III. ADDITIONAL FIGURES

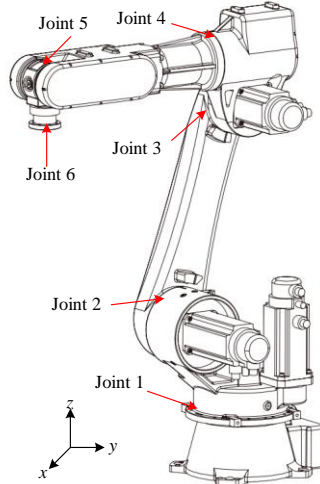
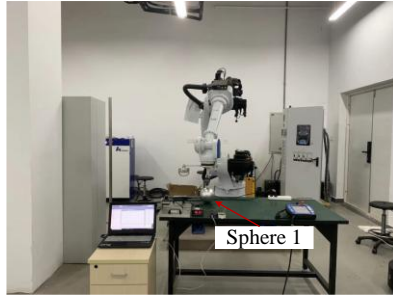
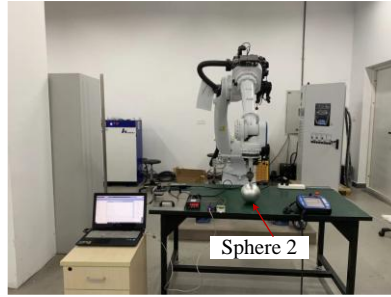


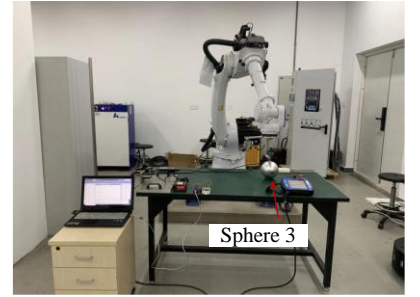
Fig. S. 1. The HSR-JR680 industrial robot. The picture originates from this website (<https://www.hsrobotics.cn/download.php>).



(a)

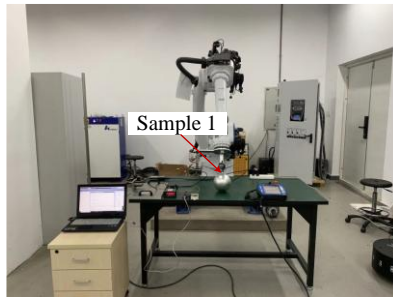


(b)

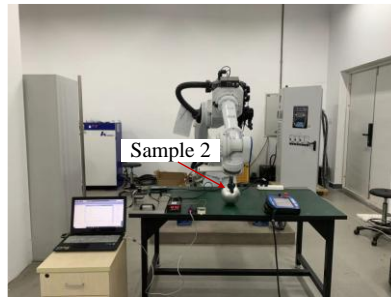


(c)

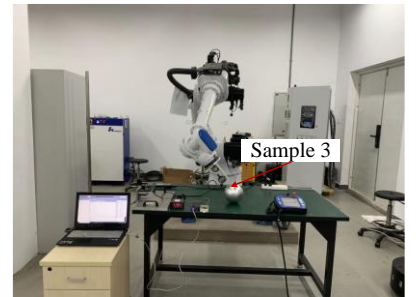
Fig. S.2. The data collection process for different spheres (D1-3). Spheres 1-3 correspond to datasets D1-3.



(a)



(b)



(c)

Fig. S.3. The data collection process at different positions on a sphere. Samples 1-3 represent three different positions on the sphere.

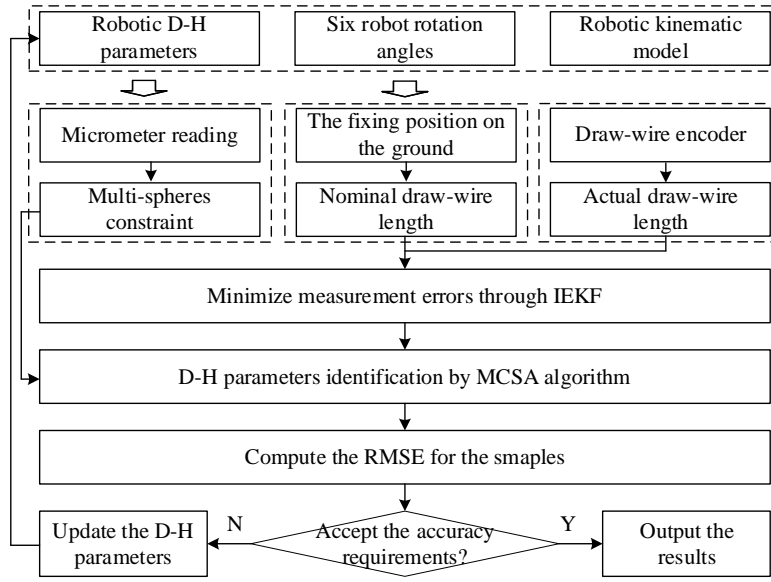
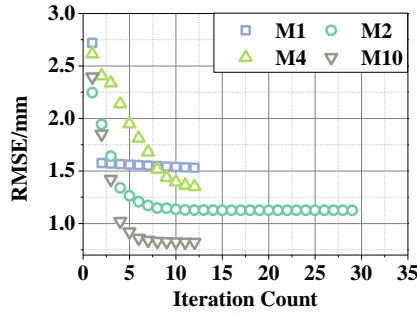
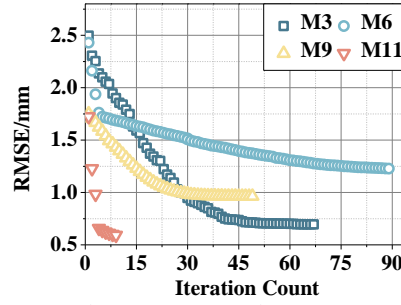


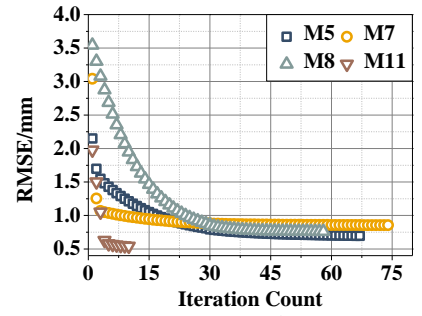
Fig. S.4. The diagram of the computational process of robot calibration.



(a) M1, M2, M4 and M10 on D1

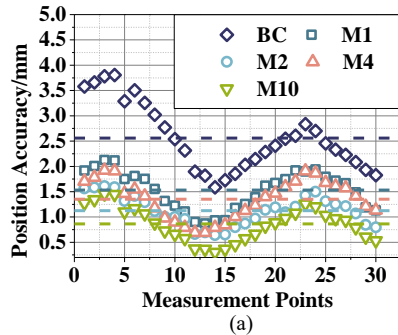


(b) M3, M6, M9 and M11 on D1

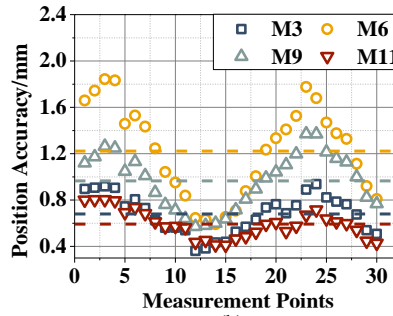


(c) M5, M7, M8 and M12 on D1

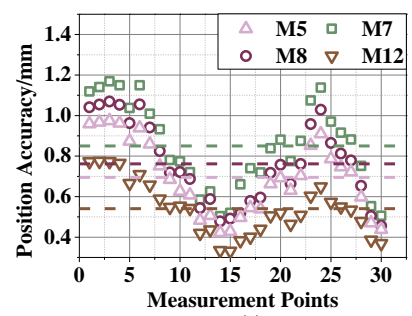
Fig. S.5. Training process of M1-12 on D1.



(a)



(b)



(c)

Fig. S.6. Positional errors of 30 samples calibrated by M1-12 on D1. (a) Positional errors of BC (before calibration) M1, M2, M4 and M10. (b) Positional errors of M3, M6, M9 and M11. (c) Positional errors of M5, M7, M8 and M12. Note that the dashed lines represent the average values. The experimental results show that among all calibrators, M12 exhibited minimal positional error.

IV. CONVERGENCE ANALYSIS OF THE MSCA ALGORITHM

Given nodes $i \in m$, and iteration t , the convergence is divided into two sequential steps:

Step 1. The difference between γ_{t+1} and γ_t is bounded by that between $(\xi_{t+1}^a, d_{1,t+1}^a)$ and $(\xi_t^a, d_{1,t}^a)$; and

Step 2. (22) is non-increasing and lower-bounded.

A. Proof of Step 1

By proving with γ as an active variable, we introduce *Lemma 1* as:

Lemma 1: Let $Y_{i,t+1} = 2[\sigma_{1,i,t}(\xi_{x,t+1} - \xi_{x,t}) + \sigma_{2,i,t}(\xi_{y,t+1} - \xi_{y,t}) + \sigma_{3,i,t}(\xi_{z,t+1} - \xi_{z,t}) + \sigma_{3,i,t}(d_{1,t+1} - d_{1,t})]$, with (28), $(\gamma_{t+1} - \gamma_t)^2$ is bounded by:

$$\begin{aligned} (\gamma_{t+1} - \gamma_t)^2 &\leq \frac{1}{\kappa^2} (\sigma_{4,i,t} - \sigma_{4,i,t-1})^2 + \kappa^2 (Y_{i,t+1} - Y_{i,t})^2 + \kappa^2 (\eta - 1)^2 [(\Phi_{i,t+1} - \Phi_{i,t}) - (\Phi_{i,t} - \Phi_{i,t-1})]^2 \\ &\quad + 4\kappa^2 [\sigma_{3,i,t}(d_{i,t+1} - d_{i,t}) - \sigma_{3,i,t-1}(d_{i,t} - d_{i,t-1})]^2 = \varpi. \end{aligned} \quad (S1)$$

Proof: Given that (21) is non-convex, any equilibrium point with a zero-gradient (e.g., a local/global optimum or a saddle point) could be a feasible solution. Considering the solution to $d_{1,t}$ by (29b) as $d_{1,t+1}$, resulting in:

$$\gamma_t = \frac{\sum \sigma_{4,i,t}}{\sum \sigma_{3,i,t}} - \frac{N\mu(d_{i,t+1} - d_{i,t})}{2\sum \sigma_{3,i,t}} - \frac{\kappa}{N} \sum (\Phi_{i,t} + Y_{i,t+1}). \quad (S2)$$

Inserting equations (29c) and (31c) into expression (S2), we can obtain:

$$\gamma_{t+1} = \frac{\sum \sigma_{4,i,t}}{\sum \sigma_{3,i,t}} - \frac{N\mu(d_{i,t+1} - d_{i,t})}{2\sum \sigma_{3,i,t}} + \frac{\kappa(1-\eta)}{N} \sum (\Phi_{i,t+1} - \Phi_{i,t}) - \frac{\kappa}{N} \sum Y_{i,t+1}. \quad (S3)$$

From the aforementioned analysis, we can infer the difference between γ_{t+1} and γ_t as:

$$\begin{aligned} \gamma_{t+1} - \gamma_t &= \left(\frac{\sum \sigma_{4,i,t}}{\sum \sigma_{3,i,t}} - \frac{\sum \sigma_{4,i,t-1}}{\sum \sigma_{3,i,t-1}} \right) - \frac{N\mu}{2} \left[\frac{(d_{i,t+1} - d_{i,t})}{\sum \sigma_{3,i,t}} - \frac{(d_{i,t} - d_{i,t-1})}{\sum \sigma_{3,i,t-1}} \right] \\ &\quad - \frac{\kappa(1-\eta)}{N} [\sum (\Phi_{i,t+1} - \Phi_{i,t}) - \sum (\Phi_{i,t} - \Phi_{i,t-1})] - \frac{\kappa}{N} \sum (Y_{i,t+1} - Y_{i,t}). \end{aligned} \quad (S4)$$

With $(a - b - c - d)^2 \leq 4(a^2 + b^2 + c^2 + d^2)$ being satisfied, we obtain:

$$\begin{aligned} (\gamma_{t+1} - \gamma_t)^2 &\leq \left(\frac{\sum \sigma_{4,i,t}}{\sum \sigma_{3,i,t}} - \frac{\sum \sigma_{4,i,t-1}}{\sum \sigma_{3,i,t-1}} \right)^2 + \frac{N^2\mu^2}{4} \left[\frac{(d_{i,t+1} - d_{i,t})}{\sum \sigma_{3,i,t}} - \frac{(d_{i,t} - d_{i,t-1})}{\sum \sigma_{3,i,t-1}} \right]^2 \\ &\quad + \frac{\kappa^2(1-\eta)^2}{N^2} [\sum (\Phi_{i,t+1} - \Phi_{i,t}) - \sum (\Phi_{i,t} - \Phi_{i,t-1})]^2 + \frac{\kappa^2}{N^2} [\sum (Y_{i,t+1} - Y_{i,t})]^2. \end{aligned} \quad (S5)$$

Based on (S5), *Lemma 1* stands. \square

B. Proof of Step 2

Lemma 2 is introduced to perform Step 2.

Lemma 2: Given the definition of the following intermediate variables, provided that the following criteria are satisfied:

$$\eta \geq 0, \kappa \geq 0, \quad (S6a)$$

$$\eta \leq 1, \kappa \geq 0, \tau \geq 0, \mu \geq 0, \quad (S6b)$$

The following inequality stands:

$$L(\xi_{t+1}, d_{1,t+1}, \gamma_{t+1}) - L(\xi_t, d_{1,t}, \gamma_t) \leq 0, \quad (S7a)$$

$$L(\xi_{t+1}, d_{1,t+1}, \gamma_{t+1}) \geq 0. \quad (S7b)$$

Proof: Considering the second-order Taylor expansion and the optimal conditions of (29a) and (31a), the difference between $L(\xi_{t+1}, d_{1,t}, \gamma_t)$ and $L(\xi_t, d_{1,t}, \gamma_t)$ is given as:

$$L(\xi_{t+1}, d_{1,t}, \gamma_t) - L(\xi_t, d_{1,t}, \gamma_t) \stackrel{(29a), (31a)}{=} \frac{4\kappa}{N} \sum_{i=1}^N \left[\sigma_{1,i,t}^2 (\xi_{x,t+1} - \xi_{x,t})^2 + \sigma_{2,i,t}^2 (\xi_{y,t+1} - \xi_{y,t})^2 + \sigma_{3,i,t}^2 (\xi_{z,t+1} - \xi_{z,t})^2 \right]. \quad (S8)$$

Similarly, according to (29b) and (31b), the difference between $L(\xi_{t+1}, d_{1,t+1}, \gamma_t)$ and $L(\xi_{t+1}, d_{1,t}, \gamma_t)$ can be described by:

$$L(\xi_{t+1}, d_{1,t+1}, \gamma_t) - L(\xi_{t+1}, d_{1,t}, \gamma_t) \stackrel{(29b), (31b)}{=} \frac{4\kappa}{N} \sum_{i=1}^N \left[\sigma_{3,i,t}^2 (d_{1,t+1} - d_{1,t})^2 \right]. \quad (S9)$$

Moreover, based on (29c), (31c) and (S1), the difference between $L(\xi_{t+1}, d_{1,t+1}, \gamma_{t+1})$ and $L(\xi_{t+1}, d_{1,t+1}, \gamma_t)$ is represented as:

$$L(\xi_{t+1}, d_{1,t+1}, \gamma_{t+1}) - L(\xi_t, d_{1,t}, \gamma_t) \stackrel{(28c), (30c)}{=} \frac{(\gamma_{t+1} - \gamma_t)^2}{\eta\kappa} \stackrel{s1}{\leq} \frac{\varpi}{\eta\kappa}. \quad (S10)$$

Combining (S7) with (S10), we can infer the following:

$$\begin{aligned} & L(\xi_{t+1}, d_{1,t+1}, \gamma_{t+1}) - L(\xi_t, d_{1,t}, \gamma_t) \\ & \leq \frac{4\kappa}{N} \sum_{i=1}^N \left[\sigma_{1,i,t}^2 (\xi_{x,t+1} - \xi_{x,t})^2 + \sigma_{2,i,t}^2 (\xi_{y,t+1} - \xi_{y,t})^2 + \sigma_{3,i,t}^2 (\xi_{z,t+1} - \xi_{z,t})^2 \right] \\ & \quad + \frac{4\kappa}{N} \sum_{i=1}^N \left[\sigma_{3,i,t}^2 (d_{1,t+1} - d_{1,t})^2 \right] \\ & \quad + \frac{1}{\eta\kappa} \left(\frac{\sum \sigma_{4,i,t}}{\sum \sigma_{3,i,t}} - \frac{\sum \sigma_{4,i,t-1}}{\sum \sigma_{3,i,t-1}} \right)^2 + \frac{N^2 \mu^2}{4\eta\kappa} \left[\frac{(d_{i,t+1} - d_{i,t})}{\sum \sigma_{3,i,t}} - \frac{(d_{i,t} - d_{i,t-1})}{\sum \sigma_{3,i,t-1}} \right]^2 \\ & \quad + \frac{\kappa(1-\eta)^2}{\eta N^2} \left[\sum (\Phi_{i,t+1} - \Phi_{i,t}) - \sum (\Phi_{i,t} - \Phi_{i,t-1}) \right]^2 + \frac{\kappa}{\eta N^2} \left[\sum (Y_{i,t+1} - Y_{i,t}) \right]^2. \end{aligned} \quad (S11)$$

$\Rightarrow \eta \geq 0, \kappa \geq 0.$

Therefore, based on the above conditions, (S6a) is satisfied, demonstrating that the augmented Lagrangian (21) does not increase. After $(t+1)$ -th iteration, (21) is rewritten as:

$$\begin{aligned} L(\xi_{t+1}, d_{1,t+1}, \gamma_{t+1}) &= \frac{1}{2N} \sum_{i=1}^N \left\| \hat{S}_i - S_i(O) \right\|_2^2 + \frac{1}{N} \sum_{i=1}^N \left\langle \Phi_i(d_{1,t+1}, \xi_{t+1}), \gamma_{t+1} \right\rangle + \frac{\kappa}{N} \sum_{i=1}^N \left[\Phi_i(d_{1,t+1}, \xi_{t+1}) \right]^2 \\ & \quad + \frac{\mu}{2} \left[(d_{1,t+1} - d_{1,t})^2 + (\xi_{x,t+1} - \xi_{x,t})^2 + (\xi_{y,t+1} - \xi_{y,t})^2 + (\xi_{z,t+1} - \xi_{z,t})^2 \right]. \end{aligned} \quad (S12)$$

By substituting (S3) into (S12), we can obtain:

$$\begin{aligned} L(\xi^{t+1}, d_1^{t+1}, \gamma^{t+1}) &= \frac{1}{2N} \sum_{i=1}^N \left\| \hat{S}_i - S_i(O) \right\|_2^2 + \frac{\kappa}{N} \sum_{i=1}^N \left[\Phi_i(d_{1,t+1}, \xi_{t+1}) \right]^2 + \tau + \frac{\kappa(1-\eta)}{N^2} \left(\sum \Phi_{i,t+1} \right)^2 \\ & \quad + \frac{\mu}{2} \left[(d_{1,t+1} - d_{1,t})^2 + (\xi_{x,t+1} - \xi_{x,t})^2 + (\xi_{y,t+1} - \xi_{y,t})^2 + (\xi_{z,t+1} - \xi_{z,t})^2 \right]. \end{aligned} \quad (S13)$$

Let $\tau = (\sum \sigma_{4,i,t} \sum \Phi_{i,t+1} / N \sum \sigma_{3,i,t}) - \mu(d_{1,t+1} - d_{1,t}) / (2 \sum \sigma_{3,i,t}) - \kappa(1-\eta) \sum \Phi_{i,t+1} \sum \Phi_{i,t+1} / N^2 - \kappa \sum \Phi_{i,t+1} \sum Y_{i,t+1} / N^2$, with (S6), (S7) and (S13) is fulfilled, i.e., (21) is lower-bounded. Consequently, *Lemma 2* stands, completing Step 2. \square

In conclusion, based on the above deductions, the implementation of Steps 1 and 2 theoretically ensures the MSCA's convergence.